

Reactions of Alkynes with [RuCl(cyclopentadienyl)] Complexes: The Important First Steps

Barnali Dutta, Basile F. E. Curchod, Pablo Campomanes, Euro Solari, Rosario Scopelliti, Ursula Rothlisberger, and Kay Severin*^[a]

Abstract: Cyclopentadienyl–ruthenium half-sandwich complexes with η^2 -bound alkyne ligands have been suggested as catalytic intermediates in the early stages of Ru-catalyzed reactions with alkynes. We show that electronically unsaturated complexes of the formula [RuCl(Cp[^])(η^2 -RC \equiv CR')] can be stabilized and crystallized by using the sterically demanding cyclopentadienyl ligand Cp[^] (Cp[^] = η^5 -1-methoxy-2,4-*tert*-butyl-3-neopentyl-cyclopentadienyl). Furthermore we demonstrate that [RuCl₂(Cp[^])₂] is an active and regioselective catalyst for the [2+2+2] cyclo-

trimerization of alkynes. The first elementary steps of the reaction of mono(η^2 -alkyne) complexes containing {RuCl(Cp[^])} (Cp[^] = η^5 -C₅Me₅) and {RuCl(Cp[^])} fragments with alkynes were investigated by DFT calculations at the M06/6-31G* level in combination with a continuum solvent model. Theoretical results are able to rational-

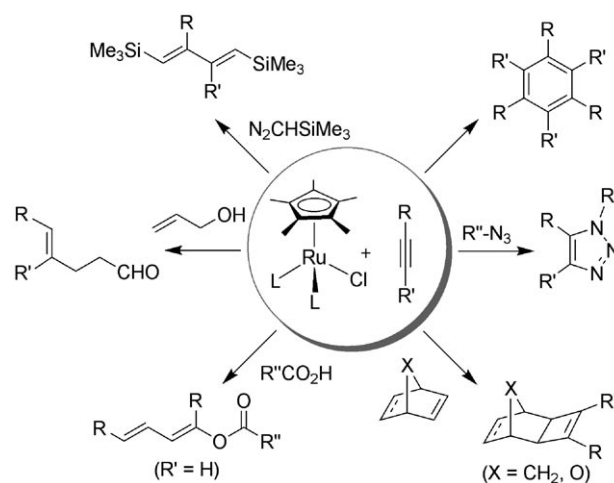
ize and complement the experimental findings. The presence of the sterically demanding Cp[^] ligand increases the activation energy required for the formation of the corresponding di(η^2 -alkyne) complexes, enhancing the initial regioselectivity, but avoiding the evolution of the system towards the expected cyclotrimerization product when bulky substituents are present. Theoretical results also show that the electronic structure and stability of a metallacyclic intermediate is strongly dependent on the nature of the substituents present in the alkyne.

Keywords: alkynes • cyclotrimerization • density functional calculations • organometallic chemistry • ruthenium

Introduction

Half-sandwich complexes containing the {RuCl(Cp[^])} fragment (Cp[^] = η^5 -C₅Me₅), such as [RuCl(cod)(Cp[^])] (cod = 1,5-cyclooctadiene), [RuCl(Cp[^])(PPh₃)₂], and [RuCl(Cp[^])₄], are potent and versatile catalysts for organic transformations involving alkynes.^[1] The catalytic reactions include the formation of arenes by [2+2+2] cyclotrimerizations,^[2] the formation of triazoles by [2+3] cycloadditions,^[3] the formation of cyclobutenes by [2+2] cycloadditions with bicyclic alkenes,^[4] the formation of dienylesters by the coupling of alkynes with carboxylic acids,^[5] the formation of γ,δ -unsatu-

rated aldehydes by reaction with allyl alcohol,^[6] and the formation of silylated 1,3-dienes by reaction with trimethylsilyldiazomethane^[7] (Scheme 1).

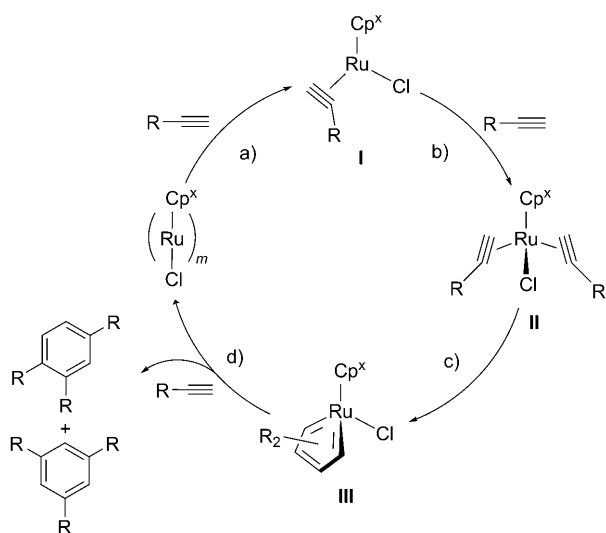


Scheme 1. [RuCl(Cp[^])(L₂)] complexes (L = PR₃, olefin) are versatile catalysts for organic transformations of alkynes.

[a] B. Dutta, B. F. E. Curchod, Dr. P. Campomanes, Dr. E. Solari, Dr. R. Scopelliti, Prof. U. Rothlisberger, Prof. K. Severin
Institut des Sciences et Ingénierie Chimiques
École Polytechnique Fédérale de Lausanne (EPFL)
1015 Lausanne (Switzerland)
Fax: (+41) 21-693-9305
E-mail: kay.severin@epfl.ch

Supporting information for this article is available on the WWW under <http://dx.doi.org/10.1002/chem.201000855>.

For most of these reactions, it is assumed that the transformation is mediated by the $\{\text{RuCl}(\text{Cp}^*)\}$ fragment and that additional ligands of the catalyst precursors, such as PPh_3 or cod , are cleaved off prior to catalysis. The generally accepted mechanism^[2,8] for the $[\text{RuCl}(\text{cyclopentadienyl})]$ -catalyzed trimerization of terminal alkynes involves η^2 -alkyne complexes of types **I** and **II** (Scheme 2). The latter



Scheme 2. Proposed mechanism for the cyclotrimerization of terminal alkynes in the presence of $[\text{RuCl}(\text{Cp})]$ catalysts.

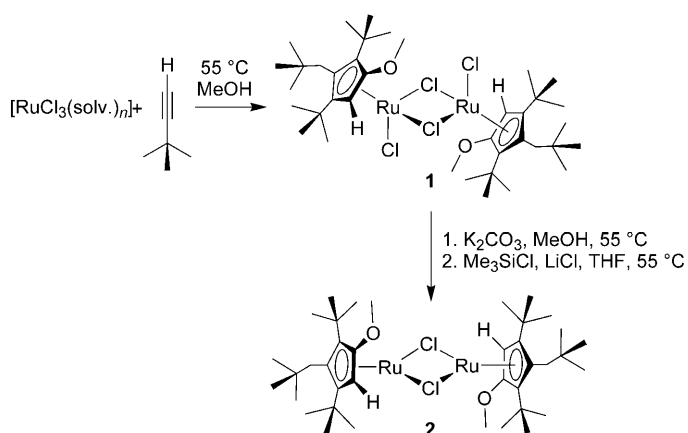
rearrange to give ruthenacyclopentatriene complexes of type **III**, which react with additional alkyne to give the aromatic $[2+2+2]$ cyclization products with regeneration of the catalytically active $[\text{RuCl}(\text{cyclopentadienyl})]_m$ species. Intermediates of type **III** have been isolated and structurally characterized,^[2,j,k,5b,9] but spectroscopic or structural data on complexes of type $[\text{RuCl}(\text{Cp}^*)(\eta^2\text{-HC}\equiv\text{CR})]$ (**I**) or $[\text{RuCl}(\text{Cp}^*)(\eta^2\text{-HC}\equiv\text{CR})_2]$ (**II**) have—to best of our knowledge—not been reported. The conversion of di(η^2 -alkyne) complexes **II** into ruthenacyclopentatriene complexes **III** (Scheme 2, step c) and the subsequent coupling reaction with alkynes (Scheme 2, step d) have both been investigated in detail by computational studies.^[2,j,8] All studies agree that the formation of the products proceeds via ruthenabicyclo-[3.2.0]heptatriene intermediates and that the rate-limiting step is the oxidative cyclization of two alkynes to give ruthenacycles **III** (Scheme 2, step c). However, most of the calculations were performed with the nonsubstituted $\{\text{RuCl}(\text{Cp})\}$ fragment ($\text{Cp}=\eta^5\text{-C}_5\text{H}_5$) and simple acetylene as the substrate, and no computations were carried out on the early steps of the reaction mechanism, that is, the conversion of the mono(η^2 -alkyne) complexes **I** into the corresponding di(η^2 -alkyne) complexes **II**.

Below we describe results of a combined experimental and theoretical study that shows that: 1) it is possible to isolate complexes of type **I**, 2) steric interactions between the π ligand and the substrate have a pronounced effect on the re-

gioselectivity of the reaction, 3) the C–C coupling process between the alkyne substrates proceeds in a stepwise fashion, and 4) the formation of di(η^2 -alkyne) complexes **II** requires a large activation energy when bulky substituents are present in both substrate and ligands thus explaining the key role played by such substituents in the reactivity of mono(η^2 -alkyne) complexes.

Results and Discussion

Recently, we have reported the synthesis of the dinuclear Ru^{II} complex $[\text{RuCl}_2(\text{Cp}^\wedge)]_2$ (**1**) ($\text{Cp}^\wedge = \eta^5\text{-1-methoxy-2,4-tert-butyl-3-neopentyl-cyclopentadienyl}$).^[10] It can be obtained in a simple one-pot reaction by heating $[\text{RuCl}_3(\text{solv.})_n]^+$ with *tert*-butyl acetylene in methanol (Scheme 3).

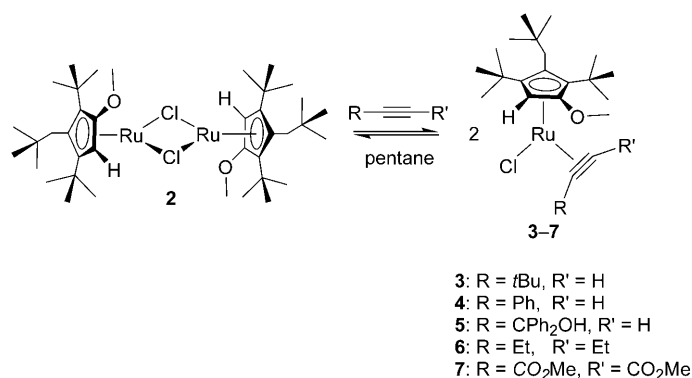


Scheme 3. Synthesis of the dinuclear complexes **1** and **2**.

Complex **1** is a structural analogue of the frequently used starting material $[\text{RuCl}_2(\text{Cp}^*)]_2$. The reactivity of complex **1** is to some extent similar to that of $[\text{RuCl}_2(\text{Cp}^*)]_2$. For example, it can easily be converted into mononuclear Ru^{II} complexes of the general formula $[\text{RuCl}(\text{Cp}^\wedge)(\text{L}_2)]$ ($\text{L} = \text{phosphines, olefins}$).^[10,11] However, the Cp^\wedge ligand is sterically more demanding than the classical Cp^* ligand. As a result, it is possible to stabilize electronically unsaturated $16e^-$ complexes, which are not accessible with the complex containing the $\{\text{Ru}(\text{Cp}^*)\}$ fragment.^[10–12] The Ru^{II} complex **2**, for example, was shown to be a chloro-bridged dimer (Scheme 3),^[12] whereas the corresponding $[\text{RuCl}(\text{Cp}^*)]$ complex is a tetramer with additional $\mu\text{-Cl}$ bridges.^[13]

The ability of the sterically demanding Cp^\wedge ligand to stabilize reactive intermediates prompted us to investigate the reactions of complexes containing the $\{\text{Ru}(\text{Cp}^\wedge)\}$ fragment with alkynes under different conditions. First, we focused on the organometallic chemistry of the dimer **2**. When an excess of *tert*-butyl acetylene was added to a pentane solution of complex **2**, an instantaneous change of the color of the solution from red to violet was observed. Cooling of the solution to -20°C led to the formation of crystals of the

monoalkyne adduct $[\text{RuCl}(\text{Cp}^*)(\eta^2\text{-HC}\equiv\text{CCMe}_3)]$ (**3**) in 61% isolated yield (Scheme 4). The structure of **3** was evidenced by X-ray crystallography (Figure 1) and elemental



Scheme 4. Synthesis of the alkyne adducts **3–7**.

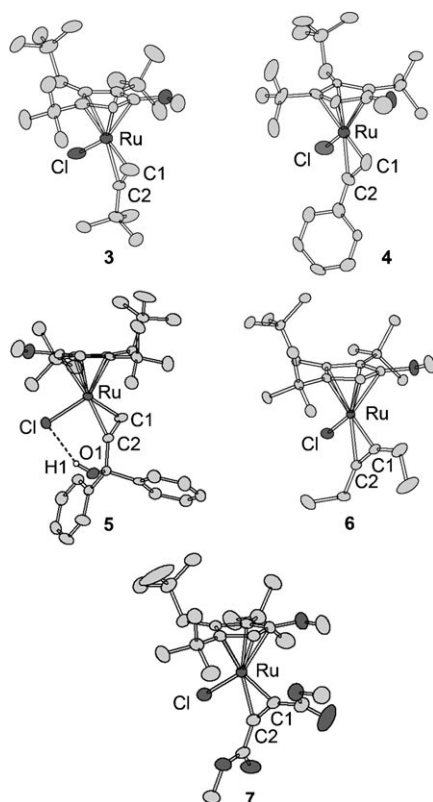


Figure 1. Molecular structures of the complexes **3–7** in the crystal. The hydrogen atoms are not shown for clarity. The thermal ellipsoids are set at 50% probability.

analysis. Complex **3** turned out to be very labile. Attempts to characterize **3** by NMR spectroscopy in solution ($[\text{D}_8]\text{toluene}$) resulted in the cleavage of the alkyne ligand and the reformation of the starting material **2**. An excess of the alkyne seems to shift the equilibrium in favor of the formation of **3**. It should be noted that alkyne trimerization was not observed, despite the fact that we have used a large

excess of *tert*-butyl acetylene. Decomposition of complex **3** also occurred when the crystals were subjected to high vacuum.

The reaction of complex **2** with phenyl acetylene in pentane gave similar results: the color of the solution turned violet upon addition of the alkyne, and crystals of the monoadduct $[\text{RuCl}(\text{Cp}^*)(\eta^2\text{-HC}\equiv\text{CPh})]$ (**4**) were obtained at low temperature. Complex **4** turned out to be even more labile than complex **3**: the solid material decomposed slowly upon storage at room temperature in the glove box. This instability precluded carrying out an elemental analysis but the structure of **4** could be established by X-ray crystallography (Figure 1). It is interesting to note that the reaction of phenylacetylene with $[\text{RuCl}(\text{cod})(\text{Cp}^*)]$ produces cleanly a ruthenacyclopentatriene complex of type **III**^[5b,9a] and not an alkyne complex as observed for $[\text{RuCl}(\text{Cp}^*)]_2$ (**2**). The difference in reactivity points to the fact that di(η^2 -alkyne) complexes of type **B** are easier to access with Cp* π ligands, a finding that is confirmed by the theoretical studies described below.

Next, we investigated the reaction of **2** with 1,1-diphenyl-2-propyn-1-ol. This alkyne is known for its tendency to form allenylidene complexes by elimination of water.^[14] However, the propargyl alcohol behaved in a similar manner to *tert*-butyl acetylene and phenyl acetylene and gave violet crystals of the monoadduct **5** in 50% isolated yield. With the internal alkynes 3-hexyne and dimethyl acetylene dicarboxylate, it was likewise possible to obtain η^2 -alkyne adducts in the form of violet crystals (**6** and **7**). For reactions with the ester, however, it was important to use only one equivalent of alkyne with respect to Ru, because an excess of alkyne lead to subsequent reactions, which are described in more detail below.

Since the solution-based characterization of the complexes **3–7** was hampered by the decomplexation of the alkyne, we have carried out crystallographic analyses for all five complexes. Graphic representations of the structures are depicted in Figure 1, and key structural parameters are summarized in Table 1. All complexes show a ‘piano-stool’ geometry with the chloride and the η^2 -bound alkyne ligand being positioned opposite to the Cp* ligand. For complexes **3–5** with terminal alkynes $\text{RC}\equiv\text{CH}$, the alkyne is coordinated in such a fashion that the R group points away from the π ligand. The asymmetry of the alkyne is reflected in the Ru–C bond lengths, with the Ru–C1 bonds being consistently shorter than the Ru–C2 bonds. For the complexes **6** and **7** with internal alkynes, the differences between the two bond

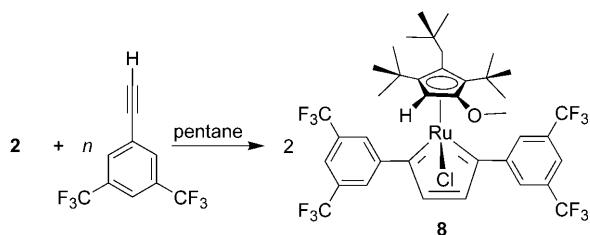
Table 1. Key bond lengths [Å] and angles [°] of complexes **3–7**

| | 3 | 4 | 5 | 6 | 7 |
|----------|-----------|-----------|-----------|-----------|-----------|
| Ru–Cl | 2.416(3) | 2.387(3) | 2.4210(9) | 2.4103(6) | 2.3897(8) |
| Ru–C1 | 2.036(13) | 1.979(12) | 2.026(4) | 2.072(2) | 2.033(3) |
| Ru–C2 | 2.123(10) | 2.082(11) | 2.095(3) | 2.101(2) | 2.058(3) |
| C1–C2 | 1.262(16) | 1.271(13) | 1.249(5) | 1.256(3) | 1.262(4) |
| C1–Ru–C2 | 35.2(5) | 36.4(4) | 35.25(14) | 35.03(8) | 35.93(12) |
| C1–C2–R | 147.2(11) | 147.6(11) | 149.3(3) | 151.8(2) | 147.9(3) |
| C2–C1–R' | 134(9) | 139(5) | 148(3) | 147.7(2) | 141.7(3) |

lengths are less pronounced. With values between 2.39 and 2.42 Å, the Ru–Cl lengths of the five complexes are similar to what has been observed for the 16e[−] complex [RuCl(Cp[∧])(PCy₃)].^[10a] The coordinated alkyne ligands are markedly bent with C1–C2–R and C2–C1–R angles between 134 and 152°. The amount of bending and the enlarged C≡C triple bond (1.26 ± 0.01 Å) is in line with what has been observed for other Ru–(η²-alkyne) complexes.^[15] For complex **5**, one can observe an internal hydrogen bond between the hydroxyl group and the chloride ligand (OH⋯Cl: 2.27, O⋯Cl: 3.056(2) Å; O–H⋯Cl: 155°).

As a representative example, complex **3** has also been characterized by ¹³C CP-MAS NMR spectroscopy in the solid state. While NMR spectroscopic studies of organometallic complexes in the solid state are not very frequent, it proved to be informative in our case. Signals for the coordinated alkyne carbons C1 and C2 were observed at δ = 130 and 158 ppm, respectively. The other carbon atoms were assigned by comparison with the ¹³C{¹H} NMR spectrum of complex **2** in solution.

When complex **2** was allowed to react with an excess of 3,5-bis(trifluoromethyl)phenylacetylene in pentane, a violet coloration indicated the formation of an η²-alkyne complex. However, on storing the solution at −20 °C for two days, we were able to isolate the ruthenacyclopentatriene complex **8** in the form of red crystals (Scheme 5).



Scheme 5. Synthesis of the ruthenacyclopentatriene complex **8**.

Evidence for the formation of a ruthenacyclopentatriene complex was obtained by crystallographic analysis (Figure 2). The coordination around the Ru center can be described as distorted tetrahedral, assuming that the Cp[∧] ligand occupies one coordination site. The description as a ruthenacyclopentatriene complex is justified by the bond

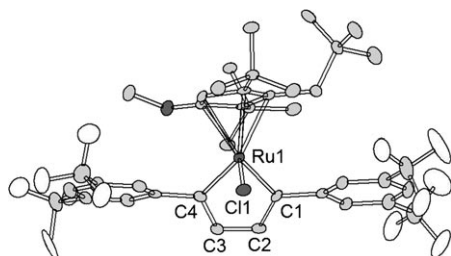


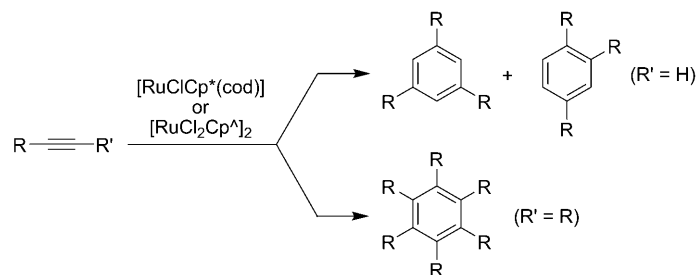
Figure 2. Molecular structures of the complex **8** in the crystal. The hydrogen atoms are not shown for clarity. The thermal ellipsoids are set at 50% probability.

lengths: with 1.406(7) and 1.427(7) Å, the C1–C2 and the C3–C4 bonds are longer than the C2–C3 bond with 1.370(8) Å. Furthermore, the Ru–C1 and the Ru–C4 bond lengths (1.997(5) and 1.976(6) Å) are in the range of a double bond. ¹⁹F NMR spectroscopy of a CD₂Cl₂ solution of crystalline **8** showed one signal indicating the formation of only one isomer. Broad and strongly temperature-dependent signals were observed in the ¹H NMR spectrum of **8** (CD₂Cl₂), possibly due to hindered rotation of the Cp[∧] ligand arising from the presence of the 3,5-bis(trifluoromethyl)arene groups. More detailed NMR spectroscopic studies were not performed as similar complexes are known with the Cp* ligand.^[2j,k,5b,9]

During our attempts to prepare alkyne complexes from the dimer [RuCl(Cp[∧])₂] (**2**) and dimethyl acetylene dicarboxylate, we observed that arenes were formed when an excess of alkyne with respect to the Ru complex was employed. This finding was not unexpected in view of the fact that [RuCl(Cp*)] complexes are known to be potent catalysts for the cyclotrimerization of electron-deficient alkynes.^[2j] To examine the catalytic behavior of the Cp[∧] complexes in more detail, we have investigated the trimerization of the terminal alkyne ethyl propiolate with catalytic amounts of complexes **1** and **2** (0.5 mol% Ru) in CD₂Cl₂. After only 10 min at room temperature, the nearly quantitative conversion of the alkyne was observed by ¹H NMR spectroscopy for both catalysts. Since the Ru^{III} complex **1** is easier to make and handle than the very sensitive Ru^{II} complex **2**, we decided to pursue all further studies with complex **1**. For comparison, we also employed the standard catalyst precursor [RuCl(cod)(Cp*)]. The results for six different alkynes are summarized in Table 2. Between 0.25 and 1.0 mol% of complex **1** (0.5–2.0 mol% Ru) were sufficient to obtain good to excellent yields of the [2+2+2] cyclotrimerization products. The catalytic activity of **1** was comparable to that of the known catalyst [RuCl(cod)(Cp*)]. However, striking differences were observed for the regioselectivity in the case of terminal alkynes. Reactions with the catalyst [RuCl(cod)(Cp*)] showed only a minor preference for the formation of the 1,2,4-isomer over the 1,3,5-isomer (~6:4). The Cp[∧] complex **1**, on the other hand, promoted the formation of the 1,2,4-isomer with excellent selectivity (≥9:1).^[16] The improved selectivity can be attributed to the increased steric demand of the Cp[∧] ligand relative to the Cp* ligand (see below). It should be noted that a related correlation between regioselectivity and steric demand of the π ligand was observed for the cycloaddition of unsymmetrical 1,6-diyne with terminal alkynes catalyzed by complexes containing {RuCl(Cp*)} and {RuCl(Cp)} fragments.^[2j]

The results presented above demonstrate that reactions of alkynes with [RuCl(Cp*)] complexes are very sensitive to the nature of both the alkyne and Cp* ligands. While MeO₂CC≡CCO₂Me gives a cyclotrimerization product, the reaction does not proceed beyond the monoalkyne adduct for *tert*-butyl acetylene. To investigate the mechanistic origin of these effects, we performed DFT/M06/6-31G* calculations of the reactions of the complexes [RuCl(Cp[∧])(η²-HC≡

Table 2. Cyclotrimerization of alkynes with the catalysts $[\text{RuCl}_2(\text{Cp}^\wedge)_2]$ and $[\text{RuCl}(\text{cod})(\text{Cp}^*)]$.^[a]



| Entry | Substrate | Catalyst [mol% Ru] | | <i>t</i> | <i>T</i> | Yield [%] ^[b] | | Product ratio 1,2,4/1,3,5 | |
|-------|---|------------------------|------------------------|----------|----------|--------------------------|------------------------|---------------------------|------------------------|
| | | {Ru(Cp [∧])} | {Ru(Cp [*])} | | | {Ru(Cp [∧])} | {Ru(Cp [*])} | {Ru(Cp [∧])} | {Ru(Cp [*])} |
| 1 | HC≡CCO ₂ Me | 0.5 | 0.5 | 10 min | RT | 98 | 98 | 92:08 | 60:40 |
| 2 | HC≡CCO ₂ Et | 0.5 | 0.5 | 30 min | RT | 97 | 96 | 90:10 | 68:32 |
| 3 | HC≡COEt | 2.0 | 2.0 | 8 h | 60°C | 70 | 92 | 93:07 | 60:40 |
| 4 | HC≡CCOMe | 0.5 | 0.5 | 20 min | RT | 99 | 76 | 94:06 | 57:43 |
| 5 | MeO ₂ CC≡CCO ₂ Me | 1.0 | 1.0 | 90 min | RT | 70 | 81 | | |
| 6 | EtO ₂ CC≡CCO ₂ Et | 1.0 | 1.0 | 3 h | RT | 75 | 85 | | |

[a] The reactions were performed in CD₂Cl₂ at RT or in 1,2-dichloroethane at 60°C. [b] The yields are based on the formation of the product as determined by ¹H NMR spectroscopy.

C(CH₃)₃]] and $[\text{RuCl}(\text{Cp}^\wedge)(\eta^2\text{-MeO}_2\text{CC}\equiv\text{CCO}_2\text{Me})]$ (**3** and **7**) with a second molecule of the corresponding alkyne. The same reaction has been studied for the Cp^{*} complex $[\text{RuCl}(\text{Cp}^*)(\eta^2\text{-HC}\equiv\text{C}(\text{CH}_3)_3)]$ (**9**) to understand the effects induced by the sterically demanding Cp[∧] ligand.

As a first test of the performance of our computational scheme, the M06/6-31G* -optimized geometries of the monoalkyne complexes $[\text{RuCl}(\text{Cp}^\wedge)(\eta^2\text{-HC}\equiv\text{C}(\text{CH}_3)_3)]$ (**3**) and $[\text{RuCl}(\text{Cp}^\wedge)(\eta^2\text{-MeO}_2\text{CC}\equiv\text{CCO}_2\text{Me})]$ (**7**) were validated with the available X-ray structures. The theoretical results are in excellent agreement for both bond lengths and angles (Table 3).^[17] Furthermore, the M06/6-31G* calculations ac-

Table 3. Computationally and experimentally determined bond lengths [Å] and angles [°] for the complexes **3** and **7**.

| | 3 (calcd) | 3 (exptl.) | 7 (calcd) | 7 (exptl.) |
|----------|------------------|-------------------|------------------|-------------------|
| Ru–Cl | 2.45 | 2.416(3) | 2.44 | 2.3897(8) |
| Ru–C1 | 2.04 | 2.036(13) | 2.06 | 2.033(3) |
| Ru–C2 | 2.11 | 2.123(10) | 2.06 | 2.058(3) |
| C1–C2 | 1.28 | 1.262(16) | 1.28 | 1.262(4) |
| C1–Ru–C2 | 35.7 | 35.2(5) | 36.2 | 35.93(12) |
| C1–C2–R | 147.1 | 147.2(11) | 153.6 | 147.9(3) |

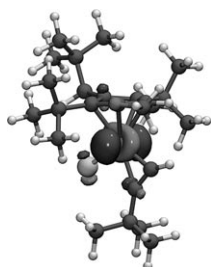


Figure 3. M06/6-31G* -optimized geometry of compound **3**. HOMO-1 is superimposed. Isovalue is set to 0.07 a.u.

curately reproduce the experimentally found orientation of the alkyne ligand. In these electronically unsaturated complexes, the plane defined by the Ru atom and the carbon atoms of the alkyne group (C1, C2) is oriented perpendicular to the plane defined by cyclopentadienyl ligand (see Figures 1 and 3), which is in contrast to what is observed for electronically

saturated $[\text{Ru}(\text{alkyne})(\text{Cp})(\text{L}_2)]$ complexes.^[15a] The orientation adopted by the alkyne moiety is optimal for avoiding “four-electron” destabilizing interactions between the doubly occupied π orbital of the alkyne and the filled d_z² orbital localized on the Ru atom (see Figure 3) while maintaining maximal overlap with the other metal orbitals.

Earlier theoretical studies have focused on the reactivity of the metallacyclic intermediate **III** (Scheme 2),^[2i,8j] but the initial steps of the reaction were not examined in detail. Our experimental results show that these steps are crucial for the rate and the regioselectivity of the cyclotrimerization reaction. For this reason, we focused our investigation on the first steps of the reaction. By starting from the mono(η²-alkyne) complexes **3**, **7**, and **9**, we studied the addition reaction of another alkyne molecule and the subsequent formation of a metallacycle. The obtained free-energy profiles in solution for the three cases considered in this study are displayed in Figure 4.

According to our calculations, the reaction between $[\text{RuCl}(\text{Cp}^*)(\eta^2\text{-HC}\equiv\text{C}(\text{CH}_3)_3)]$ and HC≡C(CH₃)₃ follows a three-step mechanism. The initial coordination of the alkyne to the Ru complex leads to the formation of a pseudo-octahedral, formally 18e⁻ organometallic compound, **B**, which is 6.5 kcal mol⁻¹ less stable than the initial adduct complex **A**. The activation free-energy barrier that has to be overcome for the coordination of the second alkyne ligand is of 7.2 kcal mol⁻¹. Subsequently, **B** evolves through the TS **TS_{BC}** (14.5 kcal mol⁻¹) into the metallabicyclic intermediate **C** (−8.7 kcal mol⁻¹), which in turn yields the final metallacycle, **D**, after surmounting a free-energy barrier of 6.7 kcal mol⁻¹ corresponding to the TS **TS_{CD}**. In summary, our calculations predict that the global process leading to the formation of the metallacycle is exothermic by −12.9 kcal mol⁻¹ and is characterized by a rate-determining step that corresponds to **TS_{BC}** with a Gibbs free-energy barrier in solution of 14.5 kcal mol⁻¹ relative to **A**. Note that our computations

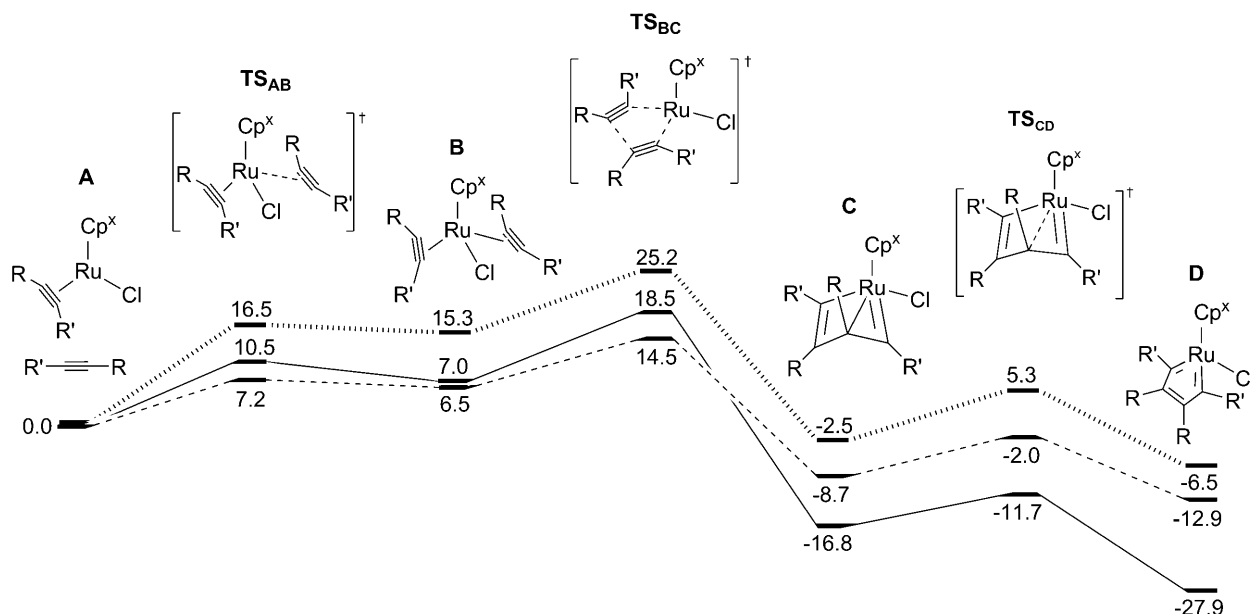


Figure 4. Gibbs-free-energy profile in dichloromethane solution for the addition of a second alkyne ligand to the complexes **3**, **7**, and **9**. Relative free energies are given in kcal mol⁻¹. -----: **9**+*tert*-butyl acetylene; —: **7**+dimethyl acetylene dicarboxylate;: **3**+*tert*-butyl acetylene.

predict a stepwise pathway for the formation of **D** from the intermediate **B**, which is in contrast with previous theoretical studies on systems with the Cp ligand and unsubstituted alkynes, in which the formation of the metallacycle from the intermediate **B** has been described as a concerted process.^[8] It appears, therefore, that the occurrence of an additional intermediate **C** is favored upon introduction of sterically demanding ligands.

To study the effect caused by the presence of the more bulky Cp[^] ligand, we investigated the corresponding free-energy reaction profile between [RuCl(Cp[^])(η^2 -HC \equiv C(CH₃)₃)] and HC \equiv C(CH₃)₃. The stationary structures located for this process (see Figure 5) are qualitatively analogous to those just described in the case of [RuCl(Cp^{*})(η^2 -HC \equiv C(CH₃)₃)]. However, with the Cp[^] ligand, the formation of the metallacycle is both kinetically and thermodynamically unfavorable. The rate-determining free-energy barrier found for the process is 10.7 kcal mol⁻¹ higher than the corresponding one in the case of the reaction between [RuCl(Cp^{*})(η^2 -HC \equiv C(CH₃)₃)] and HC \equiv C(CH₃)₃, which roughly corresponds to a decrease in the rate constant by a factor of 10⁷. Therefore, in agreement with the experimental observations, the barrier is too high to permit the evolution of the [RuCl(Cp[^])(η^2 -HC \equiv C(CH₃)₃)] complex to the metallacycle with the sterically demanding *tert*-butyl acetylene. This difference in the barriers can be mainly attributed to the presence of unfavorable steric interactions (see Figure 5) that take place between the substituents of the Cp[^] ligand and the *tert*-butyl groups of HC \equiv C(CH₃)₃. Interestingly, our computations show that a rotation of the Cp[^] ligand similar to the orientation found in the crystal structure of compound **8** (Figure 2) must take place to facilitate the formation of the metallacycle (see Figure 5). Furthermore, as already report-

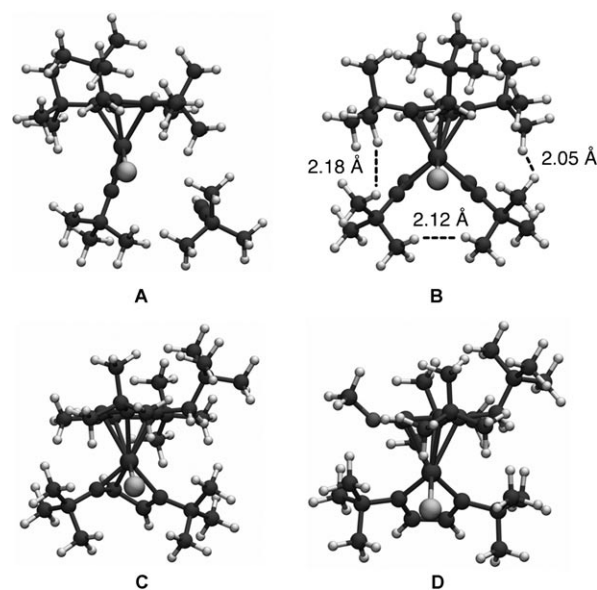


Figure 5. M06/6-31G*-optimized geometry of intermediates in the addition of *tert*-butyl acetylene to compound **3**. Short contacts are given for structure **B**.

ed in a previous study,^[8c] we observed that the orientation of the alkynes when coordinating to the Ru is strongly determined by steric effects. Addition of a second *tert*-butyl acetylene with its *tert*-butyl group in an *anti*-position with respect to the one already present in the system is indeed prohibited by the presence of the Cp[^] ligand (see Figure 6).

According to the experimental evidence presented above, the use of different alkynes leads to distinct variations of the reactivity. To investigate the possible origin of this

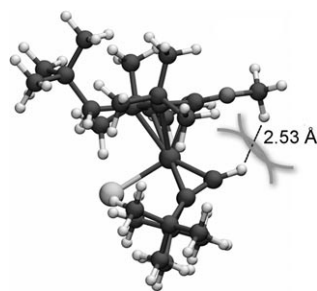


Figure 6. Side view of the M06/6-31G*-optimized geometry of intermediate **3B**. Steric interactions with the Cp^{*} π ligand would strongly disfavor an *anti* configuration of the two alkyne ligands.

effect, we also computed the corresponding free-energy profile of the addition of MeO₂CC≡CCO₂Me to [RuCl(Cp^{*})(η²-MeO₂CC≡CCO₂Me)]. The obtained profile resembles the ones previously described for the other two cases (see Figure 4) with a rate-determining energy barrier that is only ~4 kcal mol⁻¹ higher than in the case of complex **9**. No significant electronic differences were found for the stationary structures with respect to those in the other two systems we studied, once more pointing to steric interactions as the major source for the difference in barrier height. It is interesting to note that in spite of the relatively large size of the MeO₂CC≡CCO₂Me ligands, they can adopt a quasi-planar conformation that efficiently minimizes the steric interactions with the other ligands, which renders the formation of the metallacycle structure energetically feasible. The final metallacycle is much more stable in this case with the global reaction being exothermic by 27.9 kcal mol⁻¹.

Analysis of the frontier orbitals (see Figure 7) suggests that this increase in stability might be due to electronic effects. In fact, the metallacycle **7D** can be described as a ruthenacyclopentadiene, whereas those formed by complexes **3** and **9** are better described as ruthenacyclopentatrienes. The more pronounced diene character of **7D** is also evident from the carbon–carbon bond lengths of the ring (see Table 4). These electronic differences can induce variations in the reactivity of the corresponding ruthenacycles and thus have important consequences concerning the usage

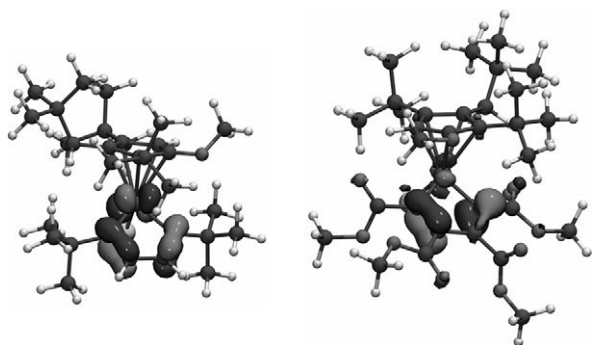


Figure 7. LUMO and HOMO-1 of the metallacycles **3D** and **7D**. Isovalues are set to 0.07 a.u.

Table 4. M06/6-31G*-selected bond lengths [Å] for the metallacycles **D** formed from complexes **3**, **7**, and **9**. See Figure 2 for notation.

| | 3 | 7 | 9 |
|-------|----------|----------|----------|
| Ru–C1 | 1.94 | 2.01 | 1.93 |
| Ru–C2 | 1.92 | 2.00 | 1.93 |
| C1–C2 | 1.44 | 1.38 | 1.44 |
| C2–C3 | 1.36 | 1.43 | 1.36 |
| C3–C4 | 1.44 | 1.37 | 1.44 |

of these complexes in the Ru-catalyzed cyclotrimerization of alkynes.

Conclusion

[Ru(η²-alkyne)_nCl(Cp)] (*n* = 1, 2) complexes have been suggested as intermediates in catalytic reactions involving [RuCl(Cp)] complexes and alkynes.^[2,8] The isolation and structural characterization of the adducts **3–7** represents, to the best of our knowledge, the first experimental evidence for complexes of this kind. The bonds between the η²-bound alkyne ligands and the {RuCl(Cp^{*})} fragment are weak, as demonstrated by the rapid dissociation of the ligand upon dissolving the complexes in organic solvents. It is interesting to note that we have not observed vinylidene complexes, although the facile η²-HC≡CR → η¹-C=CHR rearrangement is well documented for half-sandwich Ru complexes.^[15] Complex **1** was found to be an active catalyst for the [2+2+2] cyclotrimerization of alkynes. The activity of **1** was similar to that of the frequently used catalyst [RuCl(cod)(Cp^{*})], but its regioselectivity was significantly better.

The experimental results were complemented and rationalized by means of theoretical studies. The calculations show that alkyne addition to the [Ru(η²-alkyne)Cl(Cp)] complex is strongly dependent on steric effects between the alkyne and the π ligand. They also predict that the subsequent C–C coupling process to form the ruthenacycle takes place following a two-step reaction mechanism via a metallabicyclic intermediate. The higher stability of the ruthenacycle formed with electron-withdrawing alkyne substituents is due to differences appearing in the electronic structure of the system during the last step of the reaction.

Experimental Section

General: All experiments were performed inside a glove box under an atmosphere of dinitrogen containing less than 1 ppm of dioxygen and water. Thoroughly dried and deoxygenated solvents were used. The compounds RuCl₃·*n*H₂O (Precious Metals Online), *tert*-butyl acetylene (TCI), phenyl acetylene, 1,1-diphenyl-2-propyn-1-ol, dimethyl acetylene dicarboxylate, diethyl acetylene dicarboxylate, ethoxyacetylene, 3,5-bis(trifluoromethyl)phenylacetylene (Sigma–Aldrich), methyl propiolate (Maybridge), ethyl propiolate (Fluka), 3-butyne-2-one, and 3-hexyne (VWR International) were obtained from commercial suppliers. All liquid acetylenes were distilled under vacuum. ¹H and ¹³C spectra were recorded on a Bruker Avance DPX 400 and ¹⁹F NMR spectra on a Bruker AV 200 spectrometer equipped with QNP probe by using deuterated solvents. ¹³C

CP-MAS spectra were recorded on a Bruker Avance 800 MHz spectrometer at room temperature with a 2.5 mm rotor at 31.25 kHz MAS. All deuterated solvents were degassed by three freeze-pump-thaw cycles and then purified by vacuum transfer at room temperature. Fluorotrichloromethane was used as an internal standard for ^{19}F NMR spectroscopy. The complexes $[\text{RuCl}_2(\text{Cp}^\wedge)_2]$,^[10a] $[\text{RuCl}(\text{Cp}^\wedge)_2]$,^[12] and $[\text{RuCl}(\text{cod})(\text{Cp}^*)]$ ^[18] were prepared according to published procedures.

[RuCl(Cp[^])(η^2 -HC \equiv CCMe₂)] (3): An excess of *tert*-butyl acetylene (50 μL) was added to a solution of complex $[\text{RuCl}(\text{Cp}^\wedge)_2]$ (50 mg, 60 μmol) in pentane (2 mL) at RT. The color of the solution instantaneously turned violet. Crystals, appropriate for diffraction studies, appeared on keeping the solution in the freezer at -20°C for several days. The crystals were collected and kept in the glove box for few hours to eliminate the remaining traces of pentane. Yield: 37 mg (61 %); ^{13}C CP-MAS NMR (25 $^\circ\text{C}$): $\delta = 158$ (HCC*t*Bu), 130 (HCC*t*Bu), 110, 104, 94, 85 (C-Cp[^] ring), 61 (OCH₃), 59 (CH-Cp[^] ring), 38 (CH₂), 38–31 ppm (C-*t*Bu); elemental analysis calcd (%) for C₂₅H₄₃ClORu: C 60.52, H 8.74; found: C 60.13, H 8.76.

[RuCl(Cp[^])(η^2 -HC \equiv CPh)] (4): An excess of phenyl acetylene (50 μL) was added to a solution of complex $[\text{RuCl}(\text{Cp}^\wedge)_2]$ (50 mg, 60 μmol) in pentane (2 mL) at RT. The color of the solution instantaneously turned violet. A small amount of crystals, appropriate for diffraction studies, appeared on keeping the solution in the freezer at -20°C for 1 day. Complex **4** decomposed upon isolation or prolonged storage and elemental analysis was thus not performed.

[RuCl(Cp[^])(η^2 -HC \equiv CCPh₂(OH))] (5): An excess of 1,1-diphenyl-2-propyn-1-ol (50 mg) was added to a solution of complex $[\text{RuCl}(\text{Cp}^\wedge)_2]$ (50 mg, 60 μmol) in THF (0.5 mL) at RT. The color of the solution instantaneously turned violet. Pentane (2 mL) was added and the solution was placed in a freezer. Crystals, appropriate for diffraction studies, appeared on keeping the solution in the freezer at -20°C for several days. The crystals were collected and kept in the glove box for a few hours to eliminate the remaining traces of the solvent. Yield: 38 mg (50 %); elemental analysis calcd (%) for C₃₄H₄₅ClO₂Ru: C 65.63, H 7.29; found: C 65.71, H 7.15.

[RuCl(Cp[^])(η^2 -EtC \equiv CtEt)] (6): An excess of 3-hexyne (40 μL) was added to a solution of complex $[\text{RuCl}(\text{Cp}^\wedge)_2]$ (50 mg, 60 μmol) in pentane (2 mL) at RT. The color of the solution instantaneously turned violet. Crystals, appropriate for diffraction studies, appeared on keeping the solution in the freezer at -20°C for several days. The crystals were collected and kept in the glove box for few hours to eliminate the remaining traces of pentane. Yield: 38 mg (64 %); elemental analysis calcd (%) for C₂₅H₄₅ClORu: C 60.52, H 8.74; found: C 60.51, H 8.54.

[RuCl(Cp[^])(η^2 -MeOCC \equiv CCOOMe)] (7): One equivalent of dimethyl acetylene dicarboxylate (14.8 μL , 120 μmol) was added to a solution of complex $[\text{RuCl}(\text{Cp}^\wedge)_2]$ (50 mg, 60 μmol) in pentane (2 mL) at RT. The color of the solution instantaneously turned violet. Crystals, appropriate for diffraction studies, appeared on keeping the solution in the freezer at -20°C for 1 day. The crystals were collected and washed with a few drops of pentane. Yield: 47 mg (70 %); elemental analysis calcd (%) for C₂₅H₃₉ClO₅Ru: C 54.00, H 7.07; found: C 54.04, H 7.09.

[RuCl(Cp[^])(C₆H₄(CF₃)₂)-CH=CH-C(C₆H₄(CF₃)₂)] (8): An excess of 3,5-bis(trifluoromethyl)phenylacetylene (90 μL) was added to a solution of complex $[\text{RuCl}(\text{Cp}^\wedge)_2]$ (50 mg, 60 μmol) in pentane (2 mL) at RT. The color of the solution instantaneously turned violet and it was immediately cooled to -20°C . Red crystals, appropriate for diffraction studies, appeared on keeping the solution in the freezer at -20°C for 2 days. The crystals were collected and washed with pentane. Yield: 50 mg (47 %); ^{19}F NMR (CD₂Cl₂, 25 $^\circ\text{C}$): $\delta = -63.03$ ppm; elemental analysis calcd (%) for C₃₉H₄₁ClF₁₂ORu: C 52.62, H 4.64; found: C 52.73, H 4.68.

General procedure for cyclotrimerization reactions: A stock solution (12.5 mM) of the catalyst **1** was prepared in degassed CD₂Cl₂ or dichloroethane. The desired amount of the stock solution was added to a solution of the substrate containing a suitable internal standard (dioxane or *p*-xylene) (final volume = 1000 μL , substrate = 0.5 mmol). The solutions were stirred at room temperature or at 60 $^\circ\text{C}$. After a given time, a sample (20 μL) was removed from the reaction mixture, diluted with CD₂Cl₂ (350 μL), and instantaneously analyzed by ^1H NMR spectroscopy.

Crystallographic investigations: The relevant details of the crystals, data collection, and structure refinement can be found in Table 5. Diffraction data for **3**, **6**, and **8** were collected by using MoK α radiation on a 4-circle kappa goniometer equipped with a Bruker APEX II CCD at 100(2) K and all data were reduced by EvalCCD.^[19] Data collection for **4**, **5**, and **7** was performed at 140(2) K by using MoK α radiation on an Oxford Diffraction Sapphire/KM4 CCD with a kappa geometry goniometer. Data were reduced by using CrysAlis PRO.^[20] Absorption correction was applied to all data sets by using a semi-empirical method.^[21] Solution and refinement for both crystal structures were performed by SHELX.^[22] The structures were refined by using full-matrix least-squares on F^2 with all non-hydrogen atoms anisotropically defined. Hydrogen atoms were placed in calculated positions by means of a “riding” model. In some cases (**3**, **7**, and **8**), restraints have been used to treat disordered moieties or solvent. In the case of **4**, the SQUEEZE algorithm of PLATON^[23] has been used to treat very disordered solvent. Compound **8** shows an additional problem due to twinning, the law was identified [TWIN 1 0 0.5 0 -1 0 0 -1] and a BASF parameter was obtained in the last stages of refinement [0.0069(7)]. CCDC-771760–771765 contain the supplementary crystallographic data for this paper. These data can be obtained free of charge from The Cambridge Crystallographic Data Centre via www.ccdc.cam.ac.uk/data_request/cif.

Computational details: Full geometry optimizations were performed with DFT by using the M06 functional,^[24] with the relativistic effective core pseudo-potential LANL2DZ^[25] for ruthenium and the 6-31G* basis set for the remaining atoms. Remarkably, the use of more flexible basis sets including diffuse functions showed no significant changes in the main geometrical features of the optimized compounds. An ultrafine grid for the numerical evaluation of the exchange and correlation integrals and tight convergence criteria were used in all the calculations, which were carried out with the Gaussian 09 series of programs.^[26] The nature of the stationary points located was further checked, and zero-point vibrational energies (ZPVE) were evaluated by analytical computations of harmonic vibrational frequencies at the same theory level. Intrinsic reaction coordinate calculations were carried out to check the connection between the transition states (TS) and the minimum-energy structures by using the Gonzalez and Schlegel method^[27] implemented in Gaussian 09. QST computations^[28] were also employed to confirm such connections in some problematic cases. ΔG_{gas} values were calculated within the ideal gas, rigid rotor, and harmonic oscillator approximations.^[29] A pressure of 1 atm. and a temperature of 298.15 K were assumed in the calculations.

To take into account condensed-phase effects, we used a self-consistent reaction-field (SCRF) model in which the solvent is implicitly represented by a dielectric continuum characterized by its relative static dielectric permittivity ϵ . The solute, which is placed in a cavity created in the continuum after spending some cavitation energy, polarizes the continuum, which in turn creates an electric field inside the cavity. This interaction can be taken into account when using quantum chemical methods by minimizing the electronic energy of the solute plus the Gibbs energy change corresponding to the solvation process.^[30] Addition of the solvation energy to ΔG_{gas} gives the Gibbs free energy in solution, ΔG_{soln} . Within the different approaches that can be followed to calculate the electrostatic potential created by the polarized continuum in the cavity, we have employed the integral equation formalism of the polarizable continuum model (IEFPCM).^[31] The solvation Gibbs energies along the reaction coordinates were evaluated from single-point calculations on the gas-phase-optimized geometries at the same level of theory. A relative permittivity of 8.93 was employed to simulate dichloromethane as the solvent used in the experimental work.

Acknowledgements

This work was supported by the Swiss National Science Foundation and by the EPFL. The authors thank Dr. Simone Cavadini for assistance with the solid-state (CP-MAS) NMR spectroscopic measurements.

Table 5. Crystallographic data for the complexes 3–8.

| Complex | 3 | 4 | 5 | 6 | 7 | 8 |
|---|---------------------------------------|---------------------------------------|---|---------------------------------------|---|---|
| empirical formula | C ₂₅ H ₄₃ ClORu | C ₂₇ H ₃₉ ClORu | C _{37.5} H ₄₉ ClO ₂ Ru | C ₂₈ H ₄₆ ClORu | C ₂₉ H ₄₇ ClO ₆ Ru | C ₃₉ H ₄₁ ClF ₁₂ ORu |
| M _w [g mol ⁻¹] | 496.11 | 516.10 | 668.29 | 537.18 | 628.19 | 890.24 |
| crystal size [mm ³] | 0.16 × 0.13 × 0.10 | 0.38 × 0.25 × 0.12 | 0.30 × 0.25 × 0.19 | 0.25 × 0.16 × 0.13 | 0.33 × 0.30 × 0.25 | 0.26 × 0.20 × 0.09 |
| crystal system | monoclinic | monoclinic | triclinic | monoclinic | monoclinic | monoclinic |
| space group | P2 ₁ /n | I2/a | P-1 | P2 ₁ /n | P2 ₁ /c | P2 ₁ /c |
| a [Å] | 12.7932(19) | 25.363(3) | 9.6006(3) | 10.6248(10) | 15.4925(5) | 15.2196(13) |
| b [Å] | 14.4178(17) | 11.7763(9) | 12.5728(4) | 17.728(2) | 12.9986(3) | 18.4821(18) |
| c [Å] | 14.4804(19) | 37.710(3) | 15.1786(5) | 15.6814(16) | 16.1385(5) | 14.1551(18) |
| α [°] | 90 | 90 | 81.173(3) | 90 | 90 | 90 |
| β [°] | 109.589(11) | 92.085(14) | 73.336(3) | 108.889(8) | 112.418(4) | 101.153(9) |
| γ [°] | 90 | 90 | 72.131(3) | 90 | 90 | 90 |
| V [Å ³] | 2516.3(6) | 11256.2(17) | 1666.23(9) | 2794.6(5) | 3004.37(15) | 3906.5(7) |
| ρ [g cm ⁻³] | 1.310 | 1.218 | 1.332 | 1.277 | 1.389 | 1.514 |
| T [K] | 100(2) | 140(2) | 140(2) | 100(2) | 140(2) | 100(2) |
| absorption coeff. [mm ⁻¹] | 0.742 | 0.666 | 0.582 | 0.673 | 0.649 | 0.557 |
| θ range [°] | 3.29 to 25.02 | 2.43 to 25.03 | 2.81 to 26.02 | 3.58 to 27.50 | 2.73 to 26.37 | 3.31 to 27.5 |
| index ranges | -15 ≤ 15 -17 ≤ 16 -17 ≤ 17 | -30 ≤ 30 0 ≤ 14 0 ≤ 44 | -10 ≤ 11 -15 ≤ 14 -17 ≤ 18 | -13 ≤ 13 -23 ≤ 22 -20 ≤ 20 | -19 ≤ 17 -16 ≤ 16 -19 ≤ 20 | -19 ≤ 19 -23 ≤ 24 -18 ≤ 18 |
| reflns collected | 31846 | 9864 | 14755 | 62115 | 23872 | 87602 |
| independent reflns | 4425 (R _{int} =0.1294) | 9864 (R _{int} =0.0000) | 6499 (R _{int} =0.0407) | 6405 (R _{int} =0.0439) | 6088 (R _{int} =0.0399) | 8943 (R _{int} =0.1945) |
| absorption correction | semi-empirical | semi-empirical | semi-empirical | semi-empirical | semi-empirical | semi-empirical |
| max. and min. transmission | 0.928, 0.788 | 1.00000, 0.87565 | 0.895, 0.850 | 0.874, 0.738 | 0.850, 0.754 | 0.951, 0.835 |
| data/restraints/param. | 4425/13/267 | 9864/4/547 | 6499/1/383 | 6405/0/280 | 6088/5/334 | 8943/30/498 |
| GoF on F ² | 1.135 | 0.775 | 1.028 | 1.207 | 1.029 | 1.165 |
| final R indices | R1=0.1008, wR2=0.2279 | R1=0.0795, wR2=0.1442 | R1=0.0438, wR2=0.0955 | R1=0.0305, wR2=0.0571 | R1=0.0367, wR2=0.0888 | R1=0.0850, wR2=0.1139 |
| R indices (all data) | R1=0.1355, wR2=0.2458 | R1=0.2173, wR2=0.1734 | R1=0.0618, wR2=0.1001 | R1=0.0386, wR2=0.0599 | R1=0.0526, wR2=0.0948 | R1=0.1434, wR2=0.1300 |
| larg. diff. peak/hole [eÅ ⁻³] | 1.598, -1.044 | 0.581, -0.618 | 1.637, -0.527 | 0.520, -0.454 | 0.986, -0.413 | 0.921, -0.637 |

- [1] For reviews see: a) B. M. Trost, M. U. Frederiksen, M. T. Rudd, *Angew. Chem.* **2005**, *117*, 6788–6825; *Angew. Chem. Int. Ed.* **2005**, *44*, 6630–6666; b) S. Dérien, P. H. Dixneuf, *J. Organomet. Chem.* **2004**, *689*, 1382–1392; c) S. Dérien, F. Monnier, P. H. Dixneuf, *Top. Organomet. Chem.* **2004**, *11*, 1–44; d) R. Schmid, K. Kirchner, *Eur. J. Inorg. Chem.* **2004**, 2609–2626; e) C. Bruneau, *Top. Organomet. Chem.* **2004**, *11*, 125–153; f) B. M. Trost, F. D. Toste, A. B. Pinkerton, *Chem. Rev.* **2001**, *101*, 2067–2096; g) P. H. Dixneuf, C. Bruneau, S. Dérien, *Pure Appl. Chem.* **1998**, *70*, 1065–1070.
- [2] a) K. C. Nicolaou, Y. Tang, J. Wang, *Angew. Chem.* **2009**, *121*, 3501–3505; *Angew. Chem. Int. Ed.* **2009**, *48*, 3449–3453; b) L. Severa, J. Vávra, A. Kohoutová, M. Čížková, T. Šálová, J. Hývl, D. Šaman, R. Pohl, L. Adriaenssens, F. Teplý, *Tetrahedron Lett.* **2009**, *50*, 4526–4528; c) Y. Yamamoto, K. Hattori, H. Nishiyama, *J. Am. Chem. Soc.* **2006**, *128*, 8336–8340; d) Y. Yamamoto, K. Hattori, J.-i. Ishii, H. Nishiyama, *Tetrahedron* **2006**, *62*, 4294–4305; e) Y. Yamamoto, J. Ishii, H. Nishiyama, K. Itoh, *J. Am. Chem. Soc.* **2005**, *127*, 9625–9631; f) Y. Ura, Y. Sato, H. Tsujita, T. Kondo, M. Imachi, T. Mitsudo, *J. Mol. Catal. A* **2005**, *239*, 166–171; g) Y. Yamamoto, K. Kinpara, T. Saigoku, H. Nishiyama, K. Itoh, *Org. Biomol. Chem.* **2004**, *2*, 1287–1294; h) Y. Yamamoto, J. Ishii, H. Nishiyama, K. Itoh, *J. Am. Chem. Soc.* **2004**, *126*, 3712–3713; i) Y. Ura, Y. Sato, M. Shiotsuki, T. Kondo, T. Mitsudo, *J. Mol. Catal. A* **2004**, *209*, 35–39; j) Y. Yamamoto, T. Arakawa, R. Ogawa, K. Itoh, *J. Am. Chem. Soc.* **2003**, *125*, 12143–12160; k) Y. Yamamoto, K. Hata, T. Arakawa, K. Itoh, *Chem. Commun.* **2003**, 1290–1291; l) Y. Yamamoto, R. Ogawa, K. Itoh, *Chem. Commun.* **2000**, 549–550.

- [3] a) B. C. Boren, S. Narayan, L. K. Rasmussen, L. Zhang, H. Zhao, Z. Lin, G. Jia, V. V. Fokin, *J. Am. Chem. Soc.* **2008**, *130*, 8923–8930; b) U. Pradere, V. Roy, T. R. McBrayer, R. F. Schinazi, L. A. Agrofolgio, *Tetrahedron* **2008**, *64*, 9044–9051; c) L. K. Rasmussen, B. C. Boren, V. V. Fokin, *Org. Lett.* **2007**, *9*, 5337–5339; d) A. Tam, U. Arnold, M. B. Soellner, R. T. Raines, *J. Am. Chem. Soc.* **2007**, *129*, 12670–12671; e) S. Oppilliart, G. Mousseau, L. Zhang, G. Jia, P. Thuéry, B. Rousseau, J.-C. Cintrat, *Tetrahedron* **2007**, *63*, 8094–8098; f) M. M. Majireck, S. M. Weinreb, *J. Org. Chem.* **2006**, *71*, 8680–8683; g) L. Zhang, X. Chen, P. Xue, H. H. Y. Sun, I. D. Williams, B. K. Sharpless, V. V. Fokin, G. Jia, *J. Am. Chem. Soc.* **2005**, *127*, 15998–15999.
- [4] a) N. Cockburn, E. Karimi, W. Tam, *J. Org. Chem.* **2009**, *74*, 5762–5765; b) A. Allen, K. Villeneuve, N. Cockburn, E. Fatila, N. Riddell, W. Tam, *Eur. J. Org. Chem.* **2008**, 4178–4192; c) R. W. Jordan, P. Le Marquand, W. Tam, *Eur. J. Org. Chem.* **2008**, 80–86; d) R. R. Burton, W. Tam, *J. Org. Chem.* **2007**, *72*, 7333–7336; e) R. R. Burton, W. Tam, *Org. Lett.* **2007**, *9*, 3287–3290; f) A. Tenaglia, S. Gaillard, *Org. Lett.* **2007**, *9*, 3607–3610; g) P. Liu, W. Tam, J. D. Goddard, *Tetrahedron* **2007**, *63*, 7659–7666; h) K. Villeneuve, W. Tam, *Organometallics* **2006**, *25*, 843–848; i) R. W. Jordan, K. Villeneuve, W. Tam, *J. Org. Chem.* **2006**, *71*, 5830–5833; j) P. Liu, R. W. Jordan, S. P. Kibbee, J. D. Goddard, W. Tam, *J. Org. Chem.* **2006**, *71*, 3793–3803; k) R. R. Burton, W. Tam, *Tetrahedron Lett.* **2006**, *47*, 7185–7189; l) K. Villeneuve, W. Tam, *Angew. Chem.* **2004**, *116*, 620–623; *Angew. Chem. Int. Ed.* **2004**, *43*, 610–613; m) K. Villeneuve, N. Riddell, R. W. Jordan, G. C. Tsui, W. Tam, *Org. Lett.* **2004**, *6*, 4543–4546; n) R. W. Jordan, P. R. Khoury, J. D. Goddard, W.

- Tam, *J. Org. Chem.* **2004**, *69*, 8467–8474; o) R. W. Jordan, W. Tam, *Tetrahedron Lett.* **2002**, *43*, 6051–6054; p) R. W. Jordan, W. Tam, *Org. Lett.* **2001**, *3*, 2367–2370; q) R. W. Jordan, W. Tam, *Org. Lett.* **2000**, *2*, 3031–3034; r) T. Mitsudo, H. Naruse, T. Kondo, Y. Ozaki, Y. Watanabe, *Angew. Chem.* **1994**, *106*, 595–597; *Angew. Chem. Int. Ed. Engl.* **1994**, *33*, 580–581.
- [5] a) J. Le Paih, S. Dérien, B. Demerseman, C. Bruneau, P. H. Dixneuf, L. Toupet, G. Dazinger, K. Kirchner, *Chem. Eur. J.* **2005**, *11*, 1312–1324; b) J. Le Paih, F. Monnier, S. Dérien, P. H. Dixneuf, E. Clot, O. Eisenstein, *J. Am. Chem. Soc.* **2003**, *125*, 11964–11975; c) J. Le Paih, S. Dérien, P. H. Dixneuf, *Chem. Commun.* **1999**, 1437–1438.
- [6] a) S. Dérien, D. Jan, P. H. Dixneuf, *Tetrahedron* **1996**, *52*, 5511–5524; b) S. Dérien, P. H. Dixneuf, *J. Chem. Soc. Chem. Commun.* **1994**, 2551–2552; c) B. M. Trost, J. A. Flygare, *J. Org. Chem.* **1994**, *59*, 1078–1082; d) B. M. Trost, J. A. Flygare, *Tetrahedron Lett.* **1994**, *35*, 4059–4062; e) B. M. Trost, J. A. Martinez, R. J. Kulawiec, A. F. Indolese, *J. Am. Chem. Soc.* **1993**, *115*, 10402–10403; f) B. M. Trost, R. J. Kulawiec, A. Hammes, *Tetrahedron Lett.* **1993**, *34*, 587–590; g) B. M. Trost, J. A. Flygare, *J. Am. Chem. Soc.* **1992**, *114*, 5476–5477; h) B. M. Trost, R. J. Kulawiec, *J. Am. Chem. Soc.* **1992**, *114*, 5579–5584; i) B. M. Trost, G. Dyker, R. J. Kulawiec, *J. Am. Chem. Soc.* **1990**, *112*, 7809–7811.
- [7] a) F. Monnier, D. Castillo, S. Dérien, L. Toupet, P. H. Dixneuf, *Angew. Chem.* **2003**, *115*, 5632–5635; *Angew. Chem. Int. Ed.* **2003**, *42*, 5474–5477; b) J. Le Paih, S. Dérien, I. Özdemir, P. H. Dixneuf, *J. Am. Chem. Soc.* **2000**, *122*, 7400–7401.
- [8] a) J. A. Varela, C. Saá, *J. Organomet. Chem.* **2009**, *694*, 143–149; b) K. Kirchner, M. J. Calhorda, R. Schmid, L. F. Veiros, *J. Am. Chem. Soc.* **2003**, *125*, 11721–11729; c) K. Kirchner, *Monatsh. Chem.* **2008**, *139*, 337–348.
- [9] a) L. Zhang, H. H.-Y. Sung, I. D. Williams, Z. Lin, G. Jia, *Organometallics* **2008**, *27*, 5122–5129; b) Y. Yamada, J. Mizutani, M. Kurihara, H. Nishihara, *J. Organomet. Chem.* **2001**, *637–639*, 80–83; c) C. Ernst, O. Walter, E. Dinjus, *J. Organomet. Chem.* **2001**, *627*, 249–254; d) C. Ernst, O. Walter, E. Dinjus, S. Arzberger, H. Görls, *J. Prakt. Chem.* **1999**, *341*, 801–804; e) C. Gemel, A. LaPensée, K. Mauthner, K. Mereiter, R. Schmid, K. Kirchner, *Monatsh. Chem.* **1997**, *128*, 1189–1199; f) M. O. Albers, D. J. A. de Waal, D. C. Liles, D. J. Robinson, E. Singleton, M. B. Wiege, *J. Chem. Soc. Chem. Commun.* **1986**, 1680–1682.
- [10] a) B. Dutta, E. Solari, S. Gauthier, R. Scopelliti, K. Severin, *Organometallics* **2007**, *26*, 4791–4799; b) S. Gauthier, E. Solari, B. Dutta, R. Scopelliti, K. Severin, *Chem. Commun.* **2007**, 1837–1839.
- [11] B. Dutta, C. Scolaro, R. Scopelliti, P. J. Dyson, K. Severin, *Organometallics* **2008**, *27*, 4791–4799.
- [12] B. Dutta, R. Scopelliti, K. Severin, *Organometallics* **2008**, *27*, 423–429.
- [13] P. J. Fagan, W. S. Mahoney, J. C. Calabrese, I. D. Williams, *Organometallics* **1990**, *9*, 1843–1852.
- [14] M. I. Bruce, *Chem. Rev.* **1991**, *91*, 197–257.
- [15] a) E. Bustelo, J. J. Carbo, A. Lledos, K. Mereiter, M. C. Puerta, P. Valerga, *J. Am. Chem. Soc.* **2003**, *125*, 3311–3321; b) C. M. Older, J. M. Stryker, *Organometallics* **2000**, *19*, 2661–2663; c) K. Urtel, A. Frick, G. Huttner, L. Zsolnai, P. Kircher, P. Rutsch, E. Kaifer, A. Jacobi, *Eur. J. Inorg. Chem.* **2000**, 33–50; d) J. R. Lompfrey, J. P. Selegue, *J. Am. Chem. Soc.* **1992**, *114*, 5518–5523.
- [16] The regioselective formation of 1,2,4-trisubstituted benzene derivatives can be achieved with Co-based catalysts, see: G. Hilt, C. Hengst, W. Hess, *Eur. J. Org. Chem.* **2008**, 2293–2297.
- [17] In contrast, significantly distorted geometries were obtained when using the B3LYP functional. This fact is in agreement with previous theoretical investigations on similar organometallic Ru compounds that have already indicated the superior performance of M06 to capture correlation effects at the origin of the dispersion interactions between bulky ligands present in the molecular skeleton, see: a) Y. Zhao, D. G. Truhlar, *J. Chem. Theory Comput.* **2009**, *5*, 324–333; b) C. J. Cramer, D. G. Truhlar, *Phys. Chem. Chem. Phys.* **1989**, *9*, 10757–10816, and references therein.
- [18] U. Koelle, J. Kossakowski, *J. Chem. Soc. Chem. Commun.* **1988**, 549–551.
- [19] A. J. M. Duisenberg, L. M. J. Kroon-Batenburg, A. M. M. Schreurs, *J. Appl. Crystallogr.* **2003**, *36*, 220–229.
- [20] CrysAlis PRO, Oxford Diffraction Ltd., Oxfordshire, **2009**.
- [21] R. H. Blessing, *Acta Crystallogr. Sect. A* **1995**, *51*, 33–38.
- [22] SHELX: G. M. Sheldrick, *Acta Crystallogr. Sect. A* **2008**, *64*, 112–122.
- [23] PLATON, A Multipurpose Crystallographic Tool, A. L. Spek, Utrecht University, Utrecht, **2010**.
- [24] Y. Zhao, D. G. Truhlar, *Theor. Chem. Acc.* **2008**, *120*, 215–241.
- [25] P. J. Hay, W. R. Wadt, *J. Chem. Phys.* **1985**, *82*, 299–310.
- [26] Gaussian 09, Revision A.02, M. J. Frisch, G. W. Trucks, H. B. Schlegel, G. E. Scuseria, M. A. Robb, J. R. Cheeseman, G. Scalmani, V. Barone, B. Mennucci, G. A. Petersson, H. Nakatsuji, M. Caricato, X. Li, H. P. Hratchian, A. F. Izmaylov, J. Bloino, G. Zheng, J. L. Sonnenberg, M. Hada, M. Ehara, K. Toyota, R. Fukuda, J. Hasegawa, M. Ishida, T. Nakajima, Y. Honda, O. Kitao, H. Nakai, T. Vreven, J. A. Montgomery, Jr., J. E. Peralta, F. Ogliaro, M. Bearpark, J. J. Heyd, E. Brothers, K. N. Kudin, V. N. Staroverov, R. Kobayashi, J. Normand, K. Raghavachari, A. Rendell, J. C. Burant, S. S. Iyengar, J. Tomasi, M. Cossi, N. Rega, J. M. Millam, M. Klene, J. E. Knox, J. B. Cross, V. Bakken, C. Adamo, J. Jaramillo, R. Gomperts, R. E. Stratmann, O. Yazyev, A. J. Austin, R. Cammi, C. Pomelli, J. W. Ochterski, R. L. Martin, K. Morokuma, V. G. Zakrzewski, G. A. Voth, P. Salvador, J. J. Dannenberg, S. Dapprich, A. D. Daniels, Ö. Farkas, J. B. Foresman, J. V. Ortiz, J. Cioslowski, D. J. Fox, Gaussian, Inc., Wallingford CT, **2009**.
- [27] a) C. Gonzalez, H. B. Schlegel, *J. Chem. Phys.* **1989**, *90*, 2154–2161; b) C. Gonzalez, H. B. Schlegel, *J. Phys. Chem.* **1990**, *94*, 5523–5527.
- [28] C. Peng, P. Y. Ayala, H. B. Schlegel, M. J. Frisch, *J. Comput. Chem.* **1996**, *17*, 49–56.
- [29] D. A. McQuarrie, *Statistical Mechanics*, Harper, New York, **1986**.
- [30] P. Claverie in *Quantum Theory of Chemical Reactions* (Ed.: R. Daudel, A. Pullman, L. Salem, A. Veillard), Reidel, Dordrecht, **1982**.
- [31] J. Tomasi, B. Mennucci, R. Cammi, *Chem. Rev.* **2005**, *105*, 2999–3093.

Received: April 6, 2010
Published online: June 25, 2010